Polo-like kinase (Plk)1 depletion induces apoptosis in cancer cells

Xiaoqi Liu and Raymond L. Erikson*

Department of Molecular and Cellular Biology, Harvard University, Cambridge, MA 02138

Contributed by Raymond L. Erikson, March 14, 2003

Elevated expression of mammalian polo-like kinase (Plk)1 occurs in many different types of cancers, and Plk1 has been proposed as a novel diagnostic marker for several tumors. We used the recently developed vector-based small interfering RNA technique to specifically deplete Plk1 in cancer cells. We found that Plk1 depletion dramatically inhibited cell proliferation, decreased viability, and resulted in cell-cycle arrest with 4 *N* DNA content. The formation of dumbbell-like chromatin structure suggests the inability of these cells to completely separate the sister chromatids at the onset of anaphase. Plk1 depletion induced apoptosis, as indicated by the appearance of subgenomic DNA in fluorescence-activated cell-sorter (FACS) profiles, the activation of caspase 3, and the formation of fragmented nuclei. Plk1-depletion-induced apoptosis was partially reversed by cotransfection of nondegradable mouse Plk1 constructs. In addition, the p53 pathway was shown to be involved in Plk1-depletion-induced apoptosis. DNA damage occurred in Plk1-depleted cells and inhibition of ATM strongly potentiated the lethality of Plk1 depletion. Although p53 is stabilized in Plk1-depleted cells, DNA damage also occurs in $p53^{-/-}$ cells. These data support the notion that disruption of Plk1 function could be an important application in cancer therapy.

The polo kinase family includes mammalian polo-like kinase (Plk)1, Snk, Fnk, *Xenopus laevis* Plx1, *Drosophila* polo, fission yeast Plo1, and budding yeast Cdc5 (1). Genetic and biochemical experiments in various organisms indicate that polo-like kinases are important regulators of many cell-cycle-related events, including activation of Cdc2, chromosome segregation, centrosome maturation, bipolar spindle formation, regulation of anaphase-promoting complex, and execution of cytokinesis (1, 2).

To investigate the functions of Plk1 in mammalian cells, we previously directly transfected 21-nucleotide double-stranded RNA into the cells to deplete Plk1 (3). We found that Plk1 depletion results in elevated Cdc2 protein kinase activity and thus attenuates cell-cycle progression. About 45% of cells treated with Plk1 small interfering RNA (siRNA) show the formation of a dumbbell-like DNA organization, suggesting that sister chromatids are not completely separated. About 15% of these cells do complete anaphase but do not complete cytokinesis. Finally, Plk1 depletion significantly reduces centrosome amplification in hydroxyurea-treated U2OS cells (3).

A close correlation between mammalian Plk1 expression and carcinogenesis was recently documented. Mammalian Plk1 was found to be overexpressed in various human tumors, including head and neck squamous cell carcinomas, oropharyngeal carcinomas, non-small cell lung cancer, melanomas, and ovarian and endometrial carcinomas (4). It was proposed that Plk1 could be used as a novel diagnostic marker for several types of cancers (4–6). Furthermore, constitutive expression of Plk1 in NIH 3T3 cells causes oncogenic focus formation and induces tumor growth in nude mice (7). Therefore, inhibition of Plk1 function could be an important application for cancer therapy.

In our previous report, siRNA-treated cells were examined at 48 h posttransfection; however, viability was not determined (3). In this article, we took advantage of recently developed vector-based siRNA technology to specifically deplete Plk1 in cancer cells (8). This technique permitted us to characterize cells for an extended period. These new data show that Plk1 is required for cell proliferation as well as survival. The major phenotypes we observed after the depletion of Plk1 in HeLa cells are G2/M arrest and apoptosis, supported by the formation of dumbbell-like chromatin structure, and fragmented nuclei. Moreover, cotransfection of nondegradable mouse Plk1 constructs partially reversed the apoptosis phenotype. We further found that the p53 pathway is involved in Plk1-depletion-induced apoptosis. Finally, Plk1 depletion also induced apoptosis in two other cancer cell lines.

Materials and Methods

Vector Construction. Plasmid pBS/U6-Plk1 was constructed as described (8). The targeting sequence of human Plk1 (GenBank accession no. NM_005030) is GGGCGGCTTTGCCAAGTGCTT, corresponding to the coding region 183–203 relative to the first nucleotide of the start codon. Plasmid pBS/U6-Plk1-1st half (sense strand) was used as a control vector. This control vector produces RNA that cannot form a hairpin structure to generate interfering RNA.

Cell Culture and Transfections. HeLa, DU145, T98G, and GM05849 cells were maintained in DMEM (Invitrogen) supplemented with 10% (vol/vol) FBS at 37°C in an 8% CO_2/92% air atmosphere. Cells were transfected with GenePORTER reagent (GTS, San Diego) as described by the supplier. Briefly, both the DNA and GenePORTER reagent are diluted with serum-free medium by using one-half of the transfection volume. Then, the diluted DNA is added to the diluted GenePORTER reagent, mixed rapidly, and incubated at room temperature for 30 min. After the culture medium is aspirated from the 80% confluent cells seeded 1 d previously, the DNA-GenePORTER mixture is added carefully to the cells and incubated at 37°C. At 4 h posttransfection, 1 vol of medium containing 20% FBS is added and the cells are incubated overnight in 8% CO_2 at 37°C.

Plk1 Depletion. To deplete Plk1 in human cells, cells were cotransfected with pBS/U6-Plk1 and pBabe-puro at the ratio of 10:1 as described above. At 24 h posttransfection, the medium was changed, and 2 μg/ml puromycin was added to select the transfection-positive cells. After 2 d of drug selection, floating cells were washed away, and the remaining attached cells were used for phenotype analysis after additional incubation in the presence of puromycin.

Western Blotting. Transfected cells were lysed in TBSN buffer (20 mM Tris, pH 8.0/150 mM NaCl/1.5 mM EDTA/5 mM EGTA/0.5% Nonidet P-40/0.5 mM Na_3VO_4) supplemented with phosphatase and proteinase inhibitors (20 mM *p*-nitrophenyl phosphate/1 mM Pefabloc/10 μg/ml pepstatin A/10 μg/ml leupeptin/and 5 μg/ml aprotinin), and the lysates were clarified

Abbreviations: Plk1, polo-like kinase 1; siRNA, small interfering RNA; FACS, fluorescence-activated cell sorter.

*To whom correspondence should be addressed at: Department of Molecular and Cellular Biology, Harvard University, 16 Divinity Avenue, Cambridge, MA 02138. E-mail: erikson@biosun.harvard.edu.

by centrifugation at 15,000 × *g* for 30 min. Cell lysates were directly resolved by SDS/PAGE and transferred to Immobilon-P membranes (Millipore). After being blocked in TBST (20 mM Tris/137 mM NaCl/0.1% Tween 20, pH 7.6) with 5% skim milk, membranes were incubated with the primary antibodies at appropriate dilution in TBST with 3% skim milk for 2 h at room temperature. Then, membranes were washed three times with TBST solution, followed by incubation with horseradish peroxidase-linked secondary antibody (1:2,000) in TBST with 3% skim milk. Finally, membranes were visualized by enhanced chemiluminescence reagents. Anti-Plk1 monoclonal antibody was purchased from Zymed. Mouse monoclonal antibodies against caspase 3 and 8 were obtained from Santa Cruz Biotechnology and BD PharMingen, respectively. Caspase 3 antibody was diluted 1:100 before use and the antibody concentrations for Plk1 and caspase 8 were 1 and 0.5 μg/ml, respectively.

Immunofluorescence Staining. HeLa cells were grown on coverslips and cotransfected with pBS/U6-Plk1 and pBabe-puro by using GenePORTER reagent. After overnight incubation, the medium was changed and puromycin was added for 2 d before fixation. Cells were fixed with 4% paraformaldehyde for 10 min and permeabilized with methanol for 2 min. After being washed with 0.1% Triton X-100/PBS three times, cells were incubated with anti-phosphorylated histone H2AX antibody (Trevigen, Gaithersburg, MD) for 2 h at room temperature, followed by Cy3-conjugated secondary antibody incubation. Finally, DNA was stained with 4′,6-diamidino-2-phenylindole (DAPI, Sigma).

Fluorescence-Activated Cell Sorter (FACS) Analysis. Cells were harvested by trypsin digestion, washed with cold PBS, and resuspended in 75% ethanol at 4°C for at least 8 h. The fixed cells were collected by brief centrifugation and resuspended in PBS containing 200 μg/ml RNase A and 15 μg/ml propidium iodide. After incubation for 30 min at room temperature, samples were subjected to FACS.

Results

Plk1 Depletion Inhibits HeLa Cell Proliferation and Decreases Viability. To specifically deplete Plk1 in cancer cells, we took advantage of recently developed vector-based siRNA technology (8). The targeting sequence of human Plk1 is the coding region 183–203 relative to the first nucleotide of the start codon. The vector pBS/U6-Plk1 was transfected into HeLa cells, and the cells were cultured for 48 h. Cell lysates were prepared and standard Western blotting was performed. Plk1 was efficiently depleted by siRNA (Fig. 1*A Upper*), whereas the level of Erk2 was unchanged (Fig. 1*A Lower*). The level of Plk1 protein was reduced by at least 90% 48 h posttransfection, suggesting that the vector-based siRNA approach can efficiently deplete Plk1 in mammalian cells.

Because the fraction of transfected cells is not reproducible in different experiments, we developed a protocol to select a population of transfection-positive cells. As stated in *Materials and Methods*, pBabe-puro, which contains a puromycin-resistance gene, was cotransfected with pBS/U6-Plk1 to permit selection of the transfected cells. After 2 d of selection in puromycin, most untransfected cells were dead, and the surviving cells were used for phenotype analysis.

We first determined whether Plk1 depletion influences the proliferation of HeLa cells. Although transfection with the control vector did not affect the growth rate of the cells, transfection with pBS/U6-Plk1 strongly inhibited cell proliferation (Fig. 1*B*). We also examined the viability of Plk1-depleted cells. Transfection with the control vector showed very little effect on cell viability, whereas only 10% of Plk1-depleted cells were still attached to the culture dishes 6 d posttransfection (Fig. 1*C*).

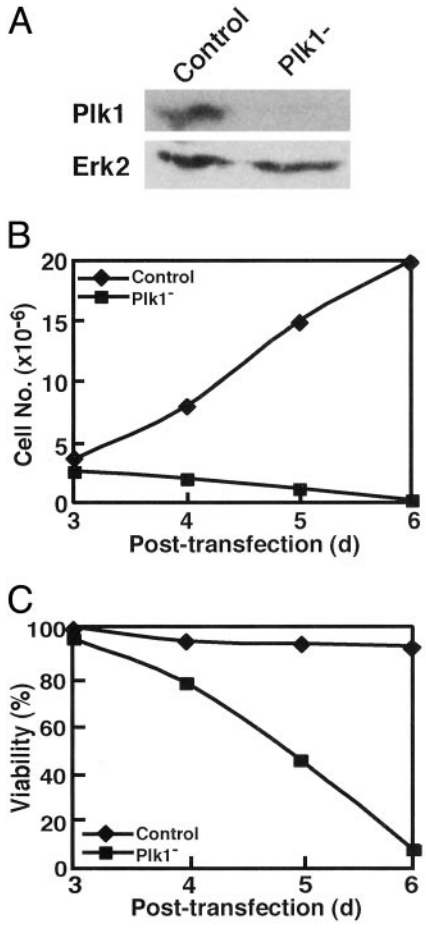

Fig. 1. Vector-based siRNA targeting Plk1. (*A*) HeLa cells were transfected with pBS/U6-Plk1 only (without cotransfection of pBabe-puro). At 2 d posttransfection, cells were harvested, and cell lysates were subjected to direct Western blotting using the antibodies as indicated on the left. (*B* and *C*) Plk1 is required for cell growth and survival. HeLa cells were transfected as described in *Materials and Methods*, and cell proliferation (*B*) and viability (*C*) were monitored. To determine cell viability, floating cells and attached cells were harvested and counted separately. Viability was calculated as the percentage of attached cells compared to total cells.

Plk1 Depletion Induces G_2/M Arrest and Apoptosis. Next, we analyzed the effect of Plk1 depletion on cell-cycle progression using FACS. As shown in Fig. 2*A*, transfection of control vector did not significantly affect the cell-cycle profile, whereas Plk1 depletion induced an obvious increase in the percentage of cells with 4*N* DNA content. At day 3 posttransfection, ≈40% of Plk1-depleted cells had a 4*N* DNA content compared with 10% in control vector-transfected cells. Moreover, the cells with sub-G1 DNA content also increased dramatically at later stages posttransfection, suggesting that Plk1-depleted cells undergo apoptosis (Fig. 2*A*). About 90% of Plk1-depleted cells displayed sub-G1 DNA at 6 d posttransfection, whereas <3% of control cells had this phenotype. To further analyze this phenotype in Plk1-depleted cells, anti-caspase 3 Western blotting was performed (Fig. 2*B Middle*). Caspase 3, the executioner caspase in apoptosis, was clearly activated, as shown by the cleavage of full-length protein. A Western blot confirmed the efficient depletion of Plk1 by the transfection with pBS/U6-Plk1 (Fig. 2*B Top*), whereas Erk2 was unchanged (Fig. 2*B Bottom*).

We also analyzed Plk1-depleted cells by confocal microscopy. At 3 d posttransfection, three populations of cells were observed (Fig. 2*C*). Chromatin was normal, dumbbell-like, or fragmented.

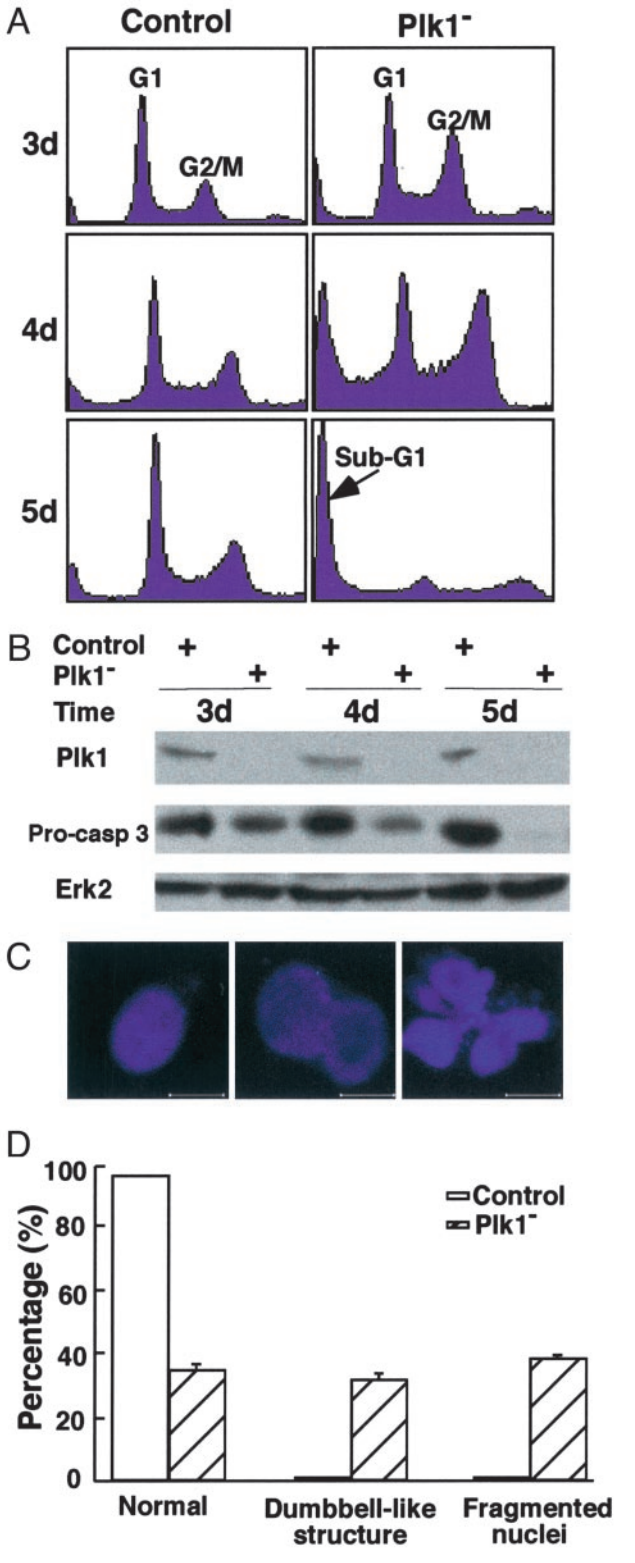

Fig. 2. Plk1 depletion induces G2/M arrest and apoptosis. After transfection as described in the text, HeLa cells were harvested and analyzed at 3, 4, or 5 d posttransfection as indicated. (*A*) FACS profiles. The positions of G1, G2/M, and sub-G1 populations are labeled. (*B*) Western blots using antibodies indicated on the left. (*C*) HeLa cells on coverslips were transfected as described. At 3 d posttransfection, the cells were fixed and DNA was stained with 4′,6-diamidino-2-phenylindole. Three typical images were normal (*Left*), dumbbell-like structure (*Center*), and fragmented nuclei (*Right*). (Scale bar: 10 μm.) (*D*) Histogram shows results from five independent experiments (>300 cells each) and bars indicate SD.

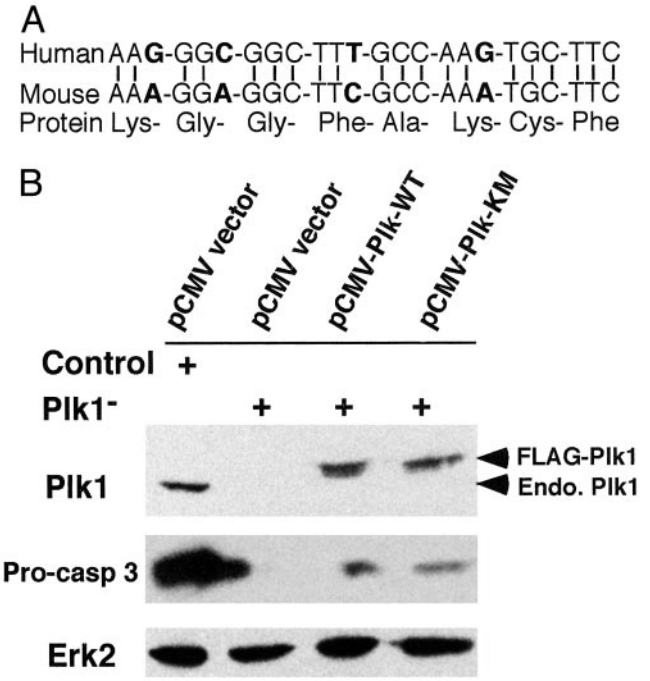

Fig. 3. Rescue of Plk1-depletion-induced apoptosis by cotransfection of mouse Plk1 constructs. (*A*) Alignment of Plk1 depletion targeting sequences. The unconserved third positions of four codons between human and mouse Plk1 sequence in the region are indicated as bold. (*B*) HeLa cells were cotransfected with pBS/U6-Plk1, one of indicated mouse Plk1 constructs and pBabe-puro at the ratio of 6:3:1 by using the protocol described in *Materials and Methods*. Cells were harvested 5 d posttransfection and cell lysates were analyzed by direct Western blotting using antibodies indicated on the left.

About 31% of Plk1-depleted cells showed dumbbell-like chromatin structure, compared with <1% of control cells. This phenotype is consistent with the obvious increase of cells with 4*N* DNA content shown in Fig. 2*A*. This observation is also in agreement with our previous report using the direct transfection of double-stranded RNA in HeLa cells to deplete Plk1. In this population of cells, analyzed at 72 h posttransfection, sister chromatids appear unable to completely separate during anaphase. About 36% of Plk1-depleted cells formed fragmented nuclei, a much higher percentage than the control cells (Fig. 2*D*). This phenotype is consistent with the appearance of a subgenomic DNA population in the FACS profile and activation of caspase 3. These data suggest Plk1-depleted cells are undergoing apoptosis.

Reversal of Apoptosis by Cotransfection of Mouse Plk1 Constructs. To confirm the above observation, we reversed the Plk1-depletion-induced events by cotransfection of mouse Plk1 constructs. As shown in Fig. 3*A*, alignment of the human Plk1 targeted sequence with mouse Plk1 sequence revealed that the third positions in four codons are not conserved. Because of the high level of specificity in RNA interfering technology, the mouse Plk1 sequence was not expected to be a target of siRNA. Indeed, cotransfection of pBS/U6-Plk1 with mouse Plk1 constructs did not affect the expression of FLAG-tagged mouse Plk1, albeit the endogenous Plk1 was completely depleted (Fig. 3*B*). Moreover, cotransfection of mouse Plk1 partially rescued the apoptotic phenotype, as indicated by the presence of a caspase 3 signal on Western blot analysis. Unexpectedly, cotransfection of kinase-defective (K82M) mouse Plk1 also showed a similar capacity to reverse, suggesting that the depletion of the Plk1 sequence itself is sufficient to cause apoptosis. An alternative explanation is that

the basal activity of the kinase-defective mutant is enough for cells to survive. As judged by casein phosphorylation, kinase-defective Plk1 has ≈15–20% of wild-type activity (unpublished data). Whether cells can survive using a Plk1-mutant that is completely dead is not known yet.

Plk1 Depletion Stabilizes p53. The p53 tumor-suppressor protein plays an important role in apoptosis and cell-cycle arrest after various stress stimuli. Consequently, we tested whether the p53 pathway was activated in Plk1-depleted cells. HeLa cells were cotransfected with pBS/U6-Plk1 and pBabe-puro, and the transfection-positive cells were selected as described in *Materials and Methods*. At day 4 posttransfection, cells were harvested and cell lysates were subjected to direct Western blotting using p53 antibody (Fig. 4*A*). The p53 level was almost undetectable in control vector-transfected cells, whereas the depletion of Plk1 dramatically increased the stability of p53.

There are two alternative pathways that initiate apoptosis: the death-receptor pathway and the mitochondrial pathway, and both pathways are affected by p53 (9). In line with the activation of p53, the expression level of Bax, a key proapoptotic protein in the mitochondrial pathway whose transcription is under control of p53 (10), was higher in Plk1-depleted cells than in control vector-transfected cells (data not shown). Activation of Bax most likely caused the subsequent activation of caspase 9, which eventually activated caspase 3 (9). We also tested the possible involvement of the death-receptor pathway in this process. As shown in Fig. 4*B*, activation of caspase 8 was observed, as indicated by the cleavage of procaspase 8 and the formation of its cleavage products (labeled by the asterisks on the left of the gel). The full-length procaspase 8 was detected as a 55/50 kDa doublet. Interestingly, it is the 50-kDa isoform that was mainly cleaved in response to Plk1 depletion (arrowhead on the right of the gel).

Because p53 activation is usually the consequence of cellular response to DNA damage, we tested whether DNA damage occurs in Plk1-depleted cells. Histone H2AX was previously shown to be hyperphosphorylated in response to DNA double-strand breaks and to colocalize with several DNA damage response proteins, including 53BP1 and Rad50 (11, 12). As shown in Fig. 4*C*, control cells do not show any phospho-H2AX staining, whereas Plk1 depletion induced strong phosphorylation and foci formation of H2AX. To determine whether DNA damage occurs before p53 activation, we further depleted p53 in Plk1$^-$ HeLa cells by cotransfection of pBS/U6-Plk1 and pSuppressor-p53, a vector designed to knockdown human p53 (Imgenex, San Diego). Strong phospho-H2AX staining was observed in these double-depleted cells (data not shown). Finally, Plk1 depletion of p53$^{-/-}$ (Saos2) cells also showed strong phospho-H2AX staining, suggesting that DNA damage is p53 independent (data not shown).

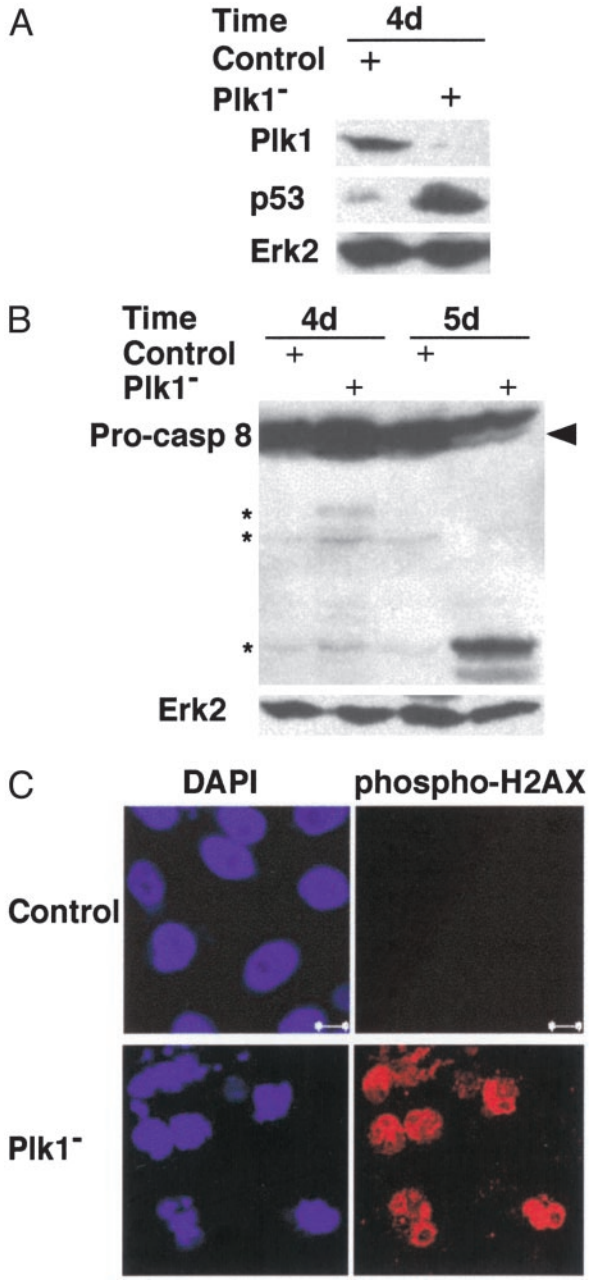

Fig. 4. p53 pathway is involved in Plk1-depletion-induced apoptosis events. (*A*) HeLa cells were transfected as described. At 4 d posttransfection, cells were harvested and cell lysates were subjected to direct Western blotting by using antibodies indicated on the left. (*B*) Plk1 in HeLa cells was depleted as described above. At indicated times posttransfection, cell lysates were analyzed by anti-caspase 8 Western blotting. Asterisks on the left indicate the positions of cleaved products of caspase 8. Arrowhead on the right indicates the full-length caspase 8 that was mainly cleaved after Plk1 depletion. (*C*) Immunofluoresence staining of Plk1-depleted cells with phospho-H2AX antibody. (Scale bar: 10 μm.)

Inhibition of ATM Potentiates the Lethality of Plk1 Depletion. Because ATM is a key player in cellular responses to DNA damage, we analyzed its role in these events by using two ATM inhibitors. Caffeine inhibits the catalytic activity of both ATM and ATR (ATM and Rad3-related) (13, 14), whereas wortmannin potently inhibits the function of ATM and phosphatidylinositol 3-kinase, but is far less efficient in inhibiting ATR function (15). As illustrated in Fig. 5, treatment of cells with either of these ATM inhibitors significantly potentiated the lethality of Plk1 depletion. In this experiment, pBabe-puro was not used for selection, and at 2 or 3 d posttransfection, cell death was not widespread (<5%). Caffeine or wortmannin treatment alone at these concentrations did not cause significant cell death. However, the addition of 2 mM caffeine or 5 μM wortmannin to Plk1-depleted cells for 1 d caused ≈40% of the cells to undergo apoptosis, and at least 60% of Plk1-depleted cells underwent apoptosis after 2 d of incubation with these drugs (Fig. 5 *A* and *B*). Because the typical transfection efficiency when GenePORTER reagent is used is 60–70%, almost every Plk1-depleted cell underwent apoptosis after 2 d exposure to ATM inhibitors.

To confirm the role of ATM in cellular response to Plk1 depletion, we examined the effect of Plk1 depletion in GM05849 cells, which are ATM deficient. We directly transfected GM05849 cells with pBS/U6-Plk1 without pBabe-puro, and

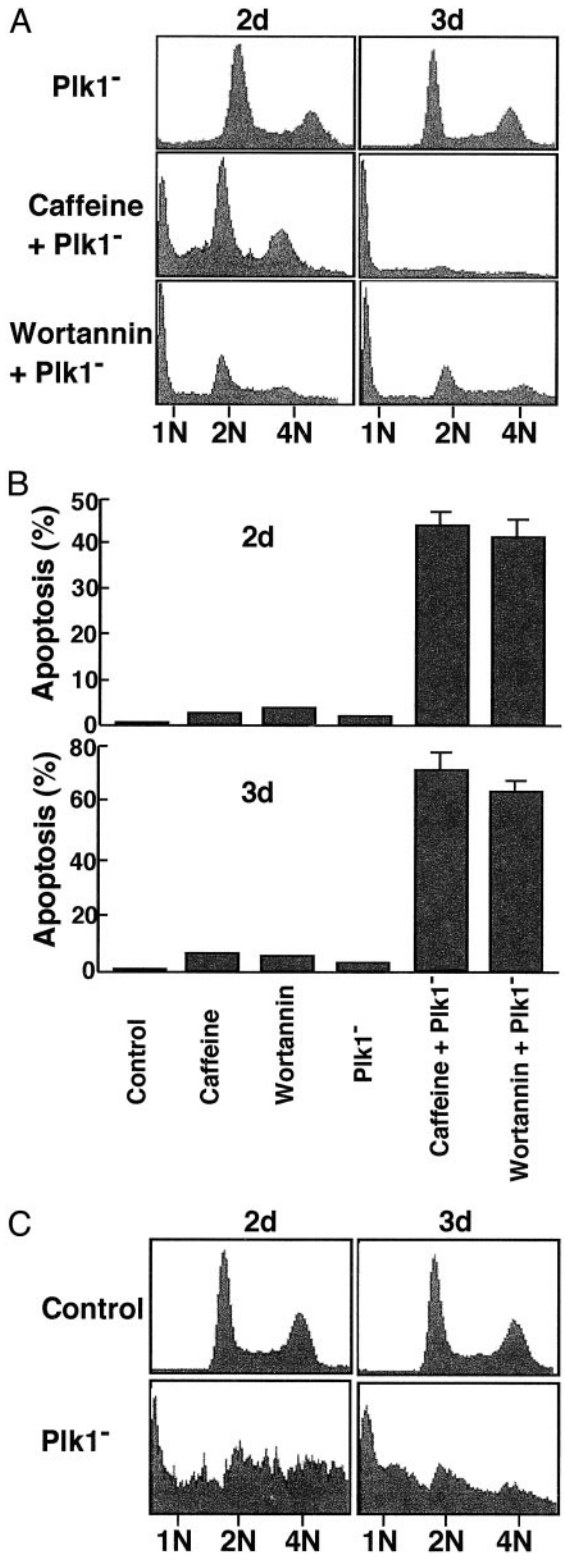

Fig. 5. ATM inhibition potentiates the lethality of Plk1 depletion. (*A* and *B*) HeLa cells were transfected with pBS/U6-Plk1 by using GenePORTER. After overnight incubation, cells were treated with either 2 mM caffeine or 5 μM wortmannin for 1 or 2 additional days. Harvested cells were subjected to FACS analysis (*A*), and percentage of apoptotic cells was calculated based on the ratio between the number of floating cells versus attached cells (*B*). (*C*) ATM$^{-/-}$ (GM05849) cells are hypersensitive to Plk1 depletion. GM05849 cells were transfected with pBS/U6-Plk1 and harvested for FACS analysis at the indicated posttransfection times. The time periods indicated in the figure are the total incubation time posttransfection.

harvested the cells for FACS analysis at day 2 or 3 posttransfection. We found that ATM$^{-/-}$ cells were extremely sensitive to Plk1 depletion. At 2 d posttransfection, ≈33% of cells displayed sub-G1 DNA and presumably underwent apoptosis. The percentage of apoptotic cells increased up to 56% by day 3 posttransfection, whereas no obvious cell death was observed for the cells that were transfected with a vector that cannot produce siRNA targeting Plk1 (Fig. 5*C*). The percentage of cell death after 3 d transfection also matched the approximate transfection efficiency when GenePORTER reagent was used.

Plk1 Depletion in Other Cancer Cell Lines. To determine whether Plk1-depletion-induced apoptosis is a general phenomenon in cancer cells, we used two other cancer cell lines: DU145 (prostate carcinoma) and T98G (brain glioblastoma multiforme). Depletion of Plk1 in both cell lines can activate caspase 3, as indicated by the decrease of full-length caspase 3 signals on Western blot analysis (data not shown).

Discussion

In this article, we report the phenotypes of human cancer cells that have been depleted of Plk1 by vector-based siRNA. Using cotransfection of a puromycin-resistance gene-containing vector, we established a protocol to obtain the maximum number of Plk1-depleted cells. We found that Plk1-depleted cells arrested at G2/M with 4N DNA content in FACS profiles and displayed a dumbbell-shaped chromatin organization as observed by confocal microscopy. The images suggest the inability of Plk1-depleted cells to completely separate the sister chromatids during mitosis. This interpretation is consistent with our previous report using direct transfection of double-stranded RNA to deplete Plk1 in HeLa cells (3). This phenotype is also supported by recent functional studies of polo-like kinases in other organisms. Cdc5, the polo-like kinase in budding yeast, has been shown to phosphorylate serine residues adjacent to cleavage sites in the cohesin subunit Scc1 and enhance its cleavage by separase before sister chromatid separation (16).

Judged by the appearance of a sub-G1 population in FACS profiles, caspase 3 activation, and the formation of fragmented nuclei, apoptosis was the second major phenotype we observed in Plk1-depleted cells 4–5 d posttransfection (Fig. 2). The fact that cotransfection of mouse Plk1 constructs partially reversed Plk1-depletion-induced apoptosis confirmed this phenotype. We expanded our study to other cancer cell lines and obtained similar phenotypes. Therefore, Plk1-depletion-induced apoptosis might be a general phenomenon in cancer cells.

The activation of p53 may be an early step in the response of cancer cells to Plk1 depletion. In the case of the death-receptor pathway, p53 activation causes up-regulation of CD95, TRAIL-R1, and TRAIL-R2, which subsequently activate caspase 8 (9). In the case of the mitochondrial pathway, active p53 transactivates proapoptotic genes such as *BAX*, *NOXA*, *PUMA*, and p53AIP1, which activate caspase 9 (9, 10). Once the two initiator caspases (8 and 9) are activated, they cleave and activate executioner caspases, mainly caspase 3. Eventually, the active caspase 3 cleaves cellular substrates to cause the characteristic biochemical and morphological changes (9).

The highly conserved C-terminal motif of histone H2AX rapidly becomes phosphorylated when cells are exposed to various stress stimuli (17, 18). The phosphorylated H2AX forms nuclear foci at the sites of DNA double-strand breaks within 1 min after exposure to ionizing radiation (17). Phosphorylation of H2AX is also an early chromatin modification event after initiation of DNA fragmentation during apoptosis (18). Thus, phospho-H2AX formation is a sensitive cellular response to various events resulting in DNA damage. In Plk1-depleted cells, DNA damage is likely the cause of p53 activation, but DNA damage appears to be a caspase 3-independent event. First, rapid

phospho-H2AX staining was detected very soon after Plk1 depletion, whereas obvious apoptosis-related events were not detected until later times after Plk1 depletion. Second, codepletion of p53 and Plk1 in HeLa cells still showed strong phospho-H2AX staining. Third, phospho-H2AX foci formation occurred in Plk1-depleted Saos2 cells, which are $p53^{-/-}$. Finally, Plk1-depleted cells were hypersensitive to ATM inhibition (see below). Thus, how Plk1 depletion induced DNA damage requires further investigation.

The use of genotoxic agents that cause DNA damage and cell death is the basis of many antitumor therapies. Both caffeine and wortmannin are radiosensitizers, which have been used to override DNA damage checkpoints to sensitize cancer cells to killing by genotoxic agents. Here, we showed that DNA damage occurred in Plk1-depleted cancer cells, presumably causing the subsequent activation of ATM and DNA damage checkpoint pathways. Activated ATM would be expected to delay onset of apoptosis; thus, Plk1-depleted cells were expected to be hypersensitive to caffeine and wortmannin treatment. The extreme sensitivity displayed by $ATM^{-/-}$ cells to Plk1 depletion also emphasized the activity of ATM protein during this process. However, although the ATM pathway is presumably activated soon after Plk1 depletion, cells eventually undergo apoptosis after prolonged Plk1 deficiency.

During the preparation of this article, another article describing the phenotypes of Plk1 depletion by using the direct transfection of several different siRNAs was published (19). In agreement with our data, Plk1 depletion of several cancer cells lines caused cell-cycle arrest at mitosis and apoptosis. We have attempted to expand our study by using human primary cells (human foreskin fibroblast 4N 46P and human lung fibroblast WI38). However, our protocol used for cancer cells did not work for primary cells, presumably because of the extremely low transfection efficiency (data not shown). More recently, by systemic administration of pBS/U6-Plk1 and the nuclease inhibitor aurintricarboxylic acid, Strebhardt and his coworkers successfully reduced Plk1 expression in neoplastic tissues and caused significant antitumor effect in human tumor xenograft mouse models (personal communication). Our studies and those of others support the premise that vector-based Plk1 depletion might be useful for cancer treatment.

We appreciate M. Michael's suggestion about the useful histone H2AX assay. We thank M. Michael, K. Strebhardt, and E. Erikson for critical reading of this manuscript. This work was supported by National Institutes of Health Grant GM59172. R.L.E. is the John F. Drum American Cancer Society Research Professor.

1. Glover, D. M., Hagan, I. M. & Tavares, A. A. M. (1998) *Genes Dev.* **12,** 3777–3787.
2. Nigg, E. A. (1998) *Curr. Opin. Cell Biol.* **10,** 776–783.
3. Liu, X. & Erikson, R. L. (2002) *Proc. Natl. Acad. Sci. USA* **99,** 8672–8676.
4. Strebhardt, K. (2001) in *PLK (Polo-Like Kinase): Encyclopedia of Molecular Medicine*, ed. Creighton, T. E. (Wiley, New York), pp. 2530–2532.
5. Knecht, R., Elez, R., Oechler, M., Solbach, C., von Ilberg, C. & Strebhardt, K. (1999) *Cancer Res.* **59,** 2794–2797.
6. Knecht, R., Oberhauser, C. & Strebhardt, K. (2000) *Int. J. Cancer* **89,** 535–536.
7. Smith, M. R., Wilson, M. L., Hamanaka, R., Chase, D., Kung, H., Longo, D. L. & Ferris, D. K. (1997) *Biochem. Biophys. Res. Commun.* **234,** 397–405.
8. Sui, G., Soohoo, C., Affar, E. B., Gay, F., Shi, Y., Forrester, W. C. & Shi, Y. (2002) *Proc. Natl. Acad. Sci. USA* **99,** 5515–5520.
9. Igney, F. H. & Krammer, P. H. (2002) *Nat. Rev.* **2,** 277–288.
10. Miyashita, T. & Reed, J. C. (1995) *Cell* **80,** 293–299.
11. Schultz, L. B., Chehab, N. H., Malikzay, A. & Halazonetis, T. D. (2000) *J. Cell Biol.* **151,** 1381–1390.
12. Paull, T. T., Rogakou, E. P., Yamazaki, V., Kirchgessner, C. U., Gellert, M. & Bonner, W. M. (2000) *Curr. Biol.* **10,** 886–895.
13. Blasina, A., Price, B. D., Turenne, G. A. & McGowan, C. H. (1999) *Curr. Biol.* **9,** 1135–1138.
14. Sarkaria, J. N., Busby, E. C., Tibbetts, R. S., Roos, P., Taya, Y., Karnitz, L. M. & Abraham, R. T. (1999) *Cancer Res.* **59,** 4375–4382.
15. Sarkaria, J. N., Tibbetts, R. S., Busby, E. C., Kennedy, A. P., Hill, D. E. & Abraham, R. T. (1998) *Cancer Res.* **58,** 4375–4382.
16. Alexandru, G., Uhlmann, F., Mechtler, K., Poupart, M. & Nasmyth, K. (2001) *Cell* **105,** 459–472.
17. Rogakou, E. P., Pilch, D. R., Orr, A. H., Ivanova, V. S. & Bonner, W. M. (1998) *J. Biol. Chem.* **273,** 5858–5868.
18. Rogakou, E. P., Nieves-Neira, W., Boon, C., Pommier, Y. & Bonner, W. M. (2000) *J. Biol. Chem.* **275,** 9390–9395.
19. Spankuch-Schmitt, B., Bereiter-Hahn, J., Kaufmann, M. & Strebhardt, K. (2002) *J. Natl. Cancer Inst.* **94,** 1863–1877.